

The impact of iodine deficiency, combined with the using of thyroid gland function influenced products, on the organs of the cardio-vascular, endocrine, and reproductive systems

Iliia V. Sobol, Oleksandra T. Harhaun, Ivan S. Kuibida, Oksana H. Popadynets

IVANO-FRANKIVSK NATIONAL MEDICAL UNIVERSITY, UKRAINE

ABSTRACT

Aim: To investigate morphofunctional changes in the endocardium, arteries' wall of different types, prostate and adrenal glands, taking into account age-related characteristics on the 60th and 90th days of iodine deficiency combined with goitrogen consumption.

Materials and Methods: The experiment was conducted on 50 white outbred male rats (25 sexually immature, 3–5 months old, and 25 sexually mature, 6–8 months old). Eleven animals from both age groups formed the control group, and 14 animals from the second and third experimental groups were subjected to simulated iodine deficiency combined with goitrogen consumption. Material collection was carried out on the 60th and 90th days of the experiment. Morphological (light and electron microscopy), morphometric, biochemical studies, and statistical data analysis were performed.

Results: On the 60th day of the experiment, the cholesterol content was: in sexually immature rats, 1.66 ± 0.19 mmol/L ($p < 0.01$); in sexually mature rats was 1.44 ± 0.15 mmol/L ($p < 0.01$). Ioduria in sexually immature animals of Group 2 was 1.42 ± 0.16 μ g/L, and in sexually mature animals it was 1.92 ± 0.21 μ g/L ($p < 0.01$). On the 90th day of the experiment, edema changes in the endocardium progressed. In light microscopy studies, the endocardium appeared as a veil-like strip covering the myocardium. In the light pink cytoplasm, flattened and weakly basophilic endothelial nuclei were visible. The content of endothelin-1 in the blood of sexually immature animals increased by 5.7% ($p < 0.05$), while in sexually mature animals, it rose by 2.4% ($p < 0.05$).

Conclusions: The level and degree of iodine deficiency is confirmed by ioduria indicators and thyroid profile. In all studied organs, edema changes develop in all constituent structures already on the 60th day of simulated iodine deficiency, progressing to the 90th day of the experiment.

KEY WORDS: endocardium, arteries, prostate gland, adrenal gland, iodine deficiency, structural and metabolic changes, postnatal ontogenesis.

Wiad Lek. 2025;78(10):1981-1987. doi: 10.36740/WLek/213591 DOI

INTRODUCTION

The level of environmental and degree and chemical influences on the functions of the endocrine glands remains an enigma due to an infinite number of potential mechanisms [1, 2, 3, 4]. Processes inhibiting the sodium/iodide symporter (NIS) and the thyroid peroxidase enzyme by certain ions contaminating water bodies have been described. These substances are known as goitrogens [5, 6].

The prostate gland can accumulate both iodide and molecular iodine. The mechanisms of iodine uptake are independent of the transporters used by the thyroid gland (i.e., not via NIS) [7]. Chronic exposure to thiourea, which blocks the conversion of thyroxine (T4) to triiodothyronine (T3) in peripheral tissues, leads to morphological and functional changes in the adrenal glands, particularly in zona fasciculata [1]. Interrelationships between the thyroid and adrenal glands under conditions of alimentary hypothyroidism are being studied [8].

Studies on rats have shown that prolonged consumption of peanut skin reduces T4 and T3 serum levels and inhibits thyroid peroxidase and 5'-deiodinase activity [9]. Adequate synthesis of thyroid hormones is critically important for maintaining cardiovascular health, as protein and enzyme synthesis required for endocardial function depend on sufficient iodine intake. This emphasizes the need for dietary adjustments in cases of iodine deficiency [10, 11, 12]. Given the prevalence of iodine deficiency and the consumption of goitrogens, along with fragmented data on their impact on the endocardium, arteries of different types, adrenal, and prostate glands, comprehensive research became necessary.

AIM

To investigate morphofunctional changes in the endocardium, arteries' wall of different types, prostate and

adrenal glands, taking into account age-related characteristics on the 60th and 90th days of iodine deficiency combined with goitrogen consumption.

MATERIALS AND METHODS

Samples of the endocardium, fragments of the aorta, external carotid, and renal arteries, prostate gland (ventral, dorsal lobes, and coagulating gland) and adrenal gland, blood, and urine were studied. Iodine deficiency was simulated according to the methodology described in [13]. Iodine deficiency combined with goitrogenic product consumption (soybeans, peanuts) was modeled based on our patented methodology [14].

The experiment was conducted on 50 white outbred male rats (25 sexually immature, 3–5 months old, and 25 sexually mature, 6–8 months old). Eleven animals from both age groups formed the control group, and 14 animals from the second and third experimental groups were subjected to simulated iodine deficiency combined with goitrogen consumption. Material collection was carried out on the 60th and 90th days of the experiment. Morphological (light and electron microscopy), morphometric, biochemical studies, and statistical data analysis were performed [15].

RESULTS AND DISCUSSION

The thyroid status of sexually immature animals in Group 1 was: TSH $0.10 \pm 0.01 \mu\text{IU/mL}$ ($p < 0.01$), T3 $3.63 \pm 0.12 \text{ nmol/L}$ ($p < 0.01$), T4 $75.44 \pm 4.01 \text{ nmol/L}$ ($p < 0.01$); in sexually mature animals: $0.08 \pm 0.00 \mu\text{IU/mL}$ ($p < 0.01$), $2.79 \pm 0.15 \text{ nmol/L}$ ($p < 0.01$), $55.18 \pm 2.72 \text{ nmol/L}$ ($p < 0.01$), respectively.

Cholesterol content under normal age conditions was: in sexually immature rats, $1.60 \pm 0.05 \text{ mmol/L}$ ($p < 0.01$); in sexually mature rats: $1.40 \pm 0.09 \text{ mmol/L}$ ($p < 0.01$). Ioduria in Group 1 sexually immature animals was $97.13 \pm 5.40 \mu\text{g/L}$, and in sexually mature animals was $101.06 \pm 3.44 \mu\text{g/L}$ ($p < 0.01$).

The thyroid status of sexually immature animals in Group 2 was as follows: TSH $0.18 \pm 0.02 \mu\text{IU/mL}$ ($p < 0.01$), T3 $3.44 \pm 0.36 \text{ nmol/L}$ ($p < 0.01$), T4 $74.40 \pm 7.10 \text{ nmol/L}$ ($p < 0.01$); in sexually mature animals: $0.14 \pm 0.01 \mu\text{IU/mL}$ ($p < 0.01$), $2.39 \pm 0.24 \text{ nmol/L}$ ($p < 0.01$), $63.60 \pm 7.46 \text{ nmol/L}$ ($p < 0.01$), respectively.

On the 60th day of the experiment, the cholesterol content was: in sexually immature rats, $1.66 \pm 0.19 \text{ mmol/L}$ ($p < 0.01$); in sexually mature rats was $1.44 \pm 0.15 \text{ mmol/L}$ ($p < 0.01$). Ioduria in sexually immature animals of Group 2 was $1.42 \pm 0.16 \mu\text{g/L}$, and in sexually mature animals it was $1.92 \pm 0.21 \mu\text{g/L}$ ($p < 0.01$).

In the light microscopic examination, the endocardium appeared as an uneven strip lining the myocardium. The nuclei of endothelial cells were not visible in all fields of view and exhibited varying basophilic intensity. The cytoplasm was weakly eosinophilic with indistinct boundaries. In ultrastructural studies, round membrane organelles were observed in the cytoplasm of endothelial cells. The luminal surface formed a

relief contour. The subendothelial layer had medium electron density. In the muscle-elastic layer, loci of optical clearance were noticeable (Fig. 1). The content of endothelin-1 in the blood of sexually immature animals increased by 4.3% ($p < 0.05$), while in sexually mature animals, it rose by 2.4% ($p < 0.05$).

In the wall of the different types of arteries, the tunics were distinguishable (Figure 1). The internal elastic membrane exhibited invaginations along the circumference of the lumen. Nuclei of endothelial cells were visible at the apexes of these invaginations. The nuclei of smooth muscle cells in the tunica media were basophilic. The adventitia exhibited localized separations. Morphometric analysis revealed that in sexually immature animals, the thickness of the aorta wall, external carotid artery, and renal artery increased by 0.9% ($p < 0.05$), 1.1% ($p < 0.05$), and 0.8% ($p < 0.05$), respectively. In sexually mature animals, this parameter increased by 0.3% ($p < 0.05$), 0.9% ($p < 0.05$), and 1.4% ($p < 0.05$), respectively.

Submicroscopic studies showed endothelial cells resting on a basal membrane, under which a subendothelial layer of different electron density was observed (Figure 1). In the clarified sarcoplasm of smooth muscle cells, mitochondria and myofilaments were visualized. Membrane organelles in fibroblasts were dilated, and connective tissue fibers were surrounded by amorphous substance.

The lumen of the terminal secretory sections of the prostate gland included homogeneous content. Epithelial cells had basally located nuclei, forming a basophilic strip. The cytoplasm was eosinophilic, with pronounced apical clearance. Blood vessels were surrounded by swollen connective tissue fibers and amorphous stromal substance (Figure 2). The height of the epithelium in the terminal secretory sections of the ventral, dorsal lobes, and coagulating gland increased by 0.5% ($p < 0.05$), 0.9% ($p < 0.05$), and 1.1% ($p < 0.05$), respectively, in sexually immature animals. In sexually mature animals, these parameters increased by 0.3% ($p < 0.05$), 0.5% ($p < 0.05$), and 1.0% ($p < 0.05$), respectively.

In ultrastructural studies, euchromatin and heterochromatin concentrated under the nucleolemma were observed in the nuclei of epithelial cells. Canals and cisternae of the granular endoplasmic reticulum, sacs, and vesicles of the endoplasmic reticulum were dilated. Myelin-like bodies were noted. The sarcoplasm of smooth muscle cells exhibited a fine-grained structure, with round mitochondria containing light matrix.

The adrenal glands demonstrated stromal and vascular wall edema in light microscopy studies. Similar edematous changes were observed in zona glomerulosa, zona fasciculata, and zona reticularis of the cortex, as well as in the medulla. Endocrine cells had light pink cytoplasm and basophilic nuclei with indistinct contours (Figure 2C). The thickness of the adrenal cortex in sexually immature animals increased by 0.4% ($p < 0.05$). In sexually mature animals, it rose by 1.6% ($p < 0.05$).

Ultrastructural studies showed light cytoplasm in endocrine cells, with round mitochondria featuring disrupted cristae and

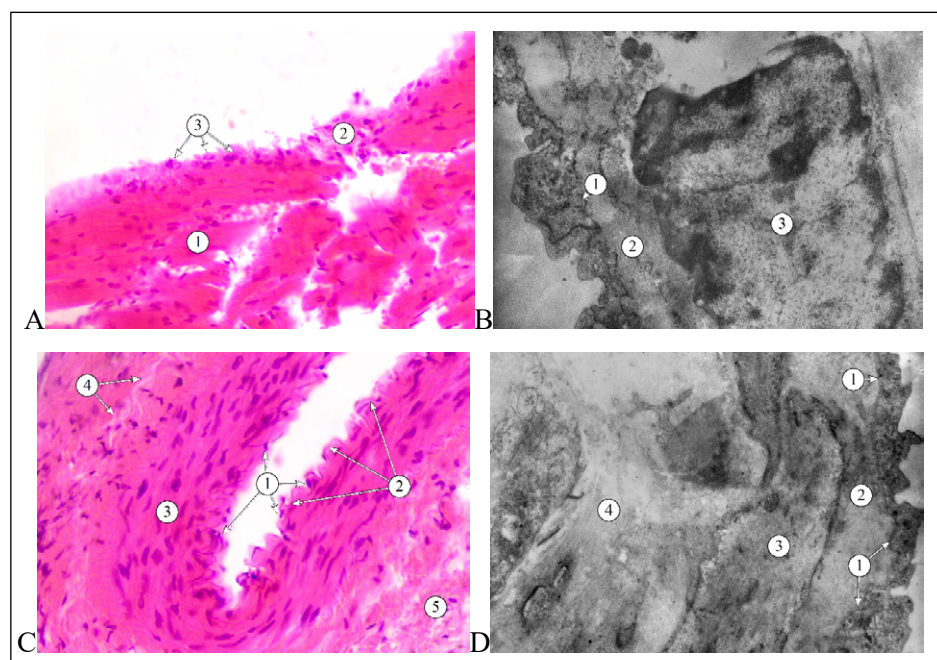


Fig. 1. Structure of the endocardium and wall of the artery on the 60th day of iodine deficiency with using of thyroid gland function influenced products. A. Endocardium of an immature animal. 1 – myocardium, 2 – endocardium, 3 – nuclei of endothelial cells. B. Endocardium of an adult animal. 1 – endothelial cell, 2 – subendothelial layer, 3 – muscular-elastic layer. C. Wall of the renal artery of an immature animal. 1 – endothelial cell nuclei, 2 – internal elastic membrane, 3 – smooth muscle cells of the media, 4 – external elastic membrane, 5 – adventitia. D – wall of the external carotid artery of a sexually mature animal. 1 – endothelial cell, 2 – subendothelial layer, 3 – smooth muscle cells, 4 – connective tissue fibers. A, C – hematoxylin and eosin, magnification: A, C x400. B, D – electron micrograph, magnification: B x9600, D x8000.

Picture taken by the authors

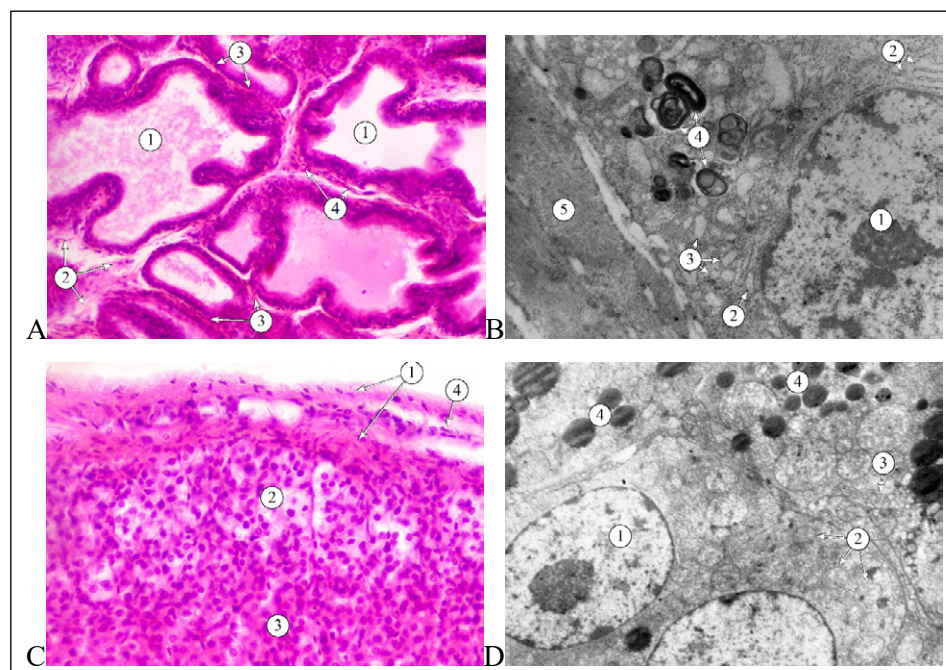


Fig. 2. Structure of the prostate and adrenal glands on the 60th day of iodine deficiency with the consumption of goiter-producing products. A. ventral lobe of the prostate gland of a sexually mature animal. 1 – terminal secretory parts, 2 – fibrous component of the stroma, 3 – smooth muscle cells of the stroma, 4 – blood vessels. B. Coagulation gland of the prostate gland of an immature animal. 1 – nucleus, 2 – granular endoplasmic reticulum, 3 – Golgi apparatus, 4 – myelin-like bodies, 5 – smooth muscle cells. C. Adrenal gland of an adult animal. 1 – capsule, 2 – zona glomerulosa, 3 – zona fasciculata, 4 – blood vessels. D – endocrine cells of the zona fasciculata of the adrenal gland of a sexually mature animal. 1 – nucleus, 2 – mitochondria, 3 – endoplasmic reticulum, 4 – lipid inclusions. A, C – hematoxylin and eosin staining, magnification: A x200, C x400. B, D – electron micrograph, magnification: B x6400, D x4800.

Picture taken by the authors

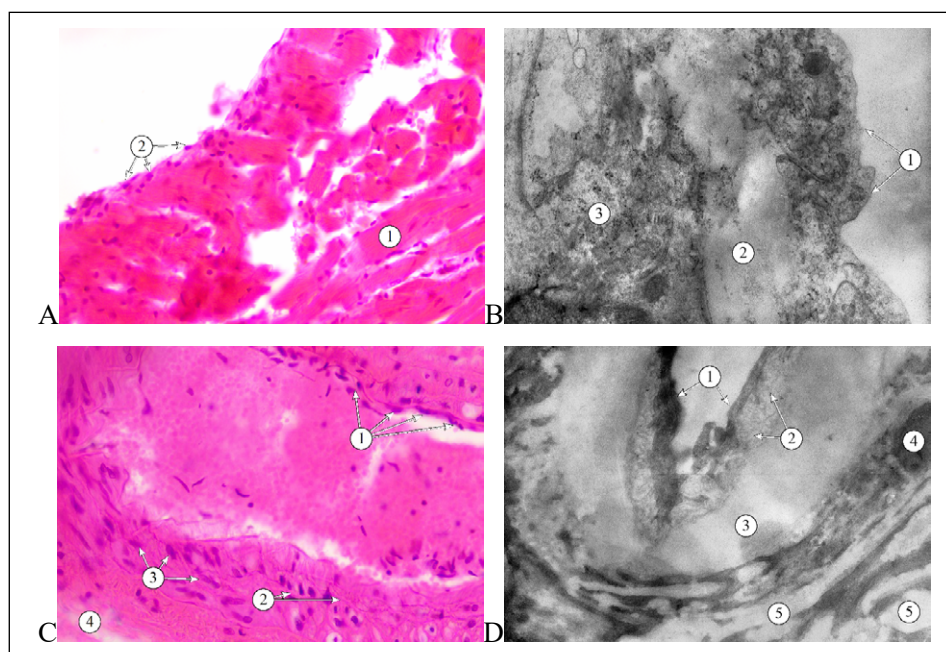


Fig. 3. Structure of the endocardium and wall of the artery on the 90th day of iodine deficiency with the consumption of goiter-producing products. A. endocardium of a sexually mature animal. 1 – myocardium, 2 – nuclei of the endothelial cells of endocardium. B. Endocardium of an immature animal. 1 – endothelial cells, 2 – subendothelial layer, 3 – muscular-elastic layer. C. Wall of the carotis externa artery. 1 – endothelial cell nuclei, 2 – connective tissue fibers of the media, 3 – smooth muscle cells of media, 5 – adventitia. D – wall of the renal artery of a sexually immature animal. 1 – endothelial cell, 2 – subendothelial layer, 3 – internal elastic membrane, 4 – smooth muscle cell, 5 – elastic fibers. A, C – hematoxylin and eosin, magnification: A, C x400. B, D – electron micrograph, magnification: B x20000, D x6400. *Picture taken by the authors*

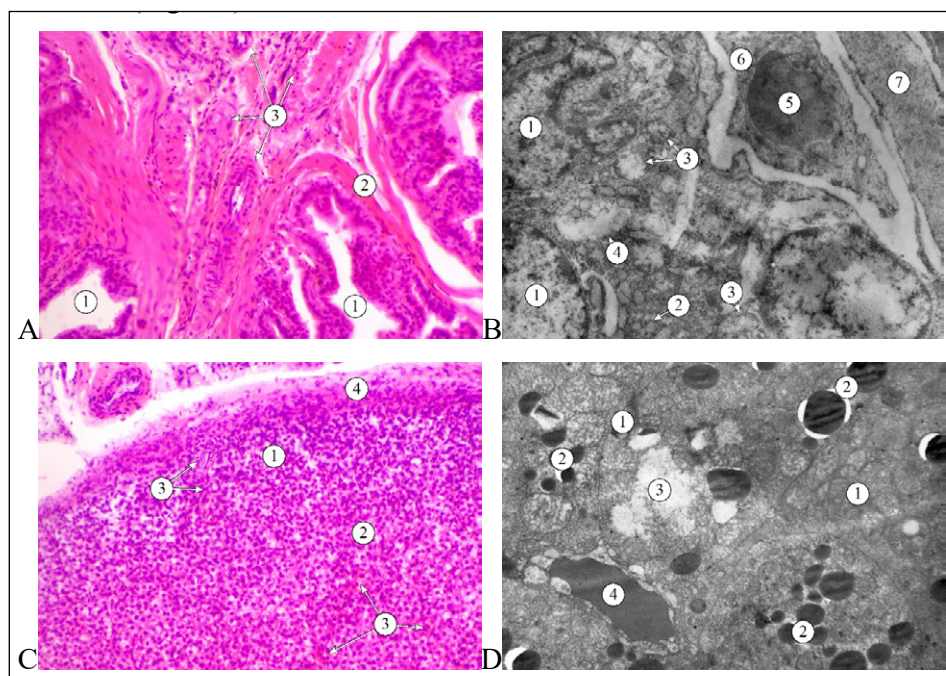


Fig. 4. Structure of the prostate and adrenal glands on the 90th day of iodine deficiency with the consumption of goiter-producing products. A. Coagulation gland of the prostate gland of an immature animal. 1 – terminal secretory sections, 2 – smooth muscle cells of the stroma, 3 – blood vessels. B. Ventral lobe of the prostate gland of a sexually mature animal. 1 – nucleus, 2 – Golgi apparatus, 3 – mitochondria, 4 – vacuoles, 5 – erythrocyte, 6 – endothelial cell, 7 – smooth muscle cell. C. adrenal gland of an immature animal. 1 – zona glomerulosa, 2 – zona fasciculata, 3 – blood vessels, 4 – capsule. D – endocrine cells of the zona fasciculata of the adrenal gland of a sexually mature animal. 1 – mitochondria, 2 – lipid inclusions, 3 – disorganized endoplasmic reticulum, 4 – erythrocyte in the lumen of the blood capillary. A, C – hematoxylin and eosin, magnification: A, C x200, B, D – electron micrograph, magnification: B x6400, D x4000. *Picture taken by the authors*

light matrix. The endoplasmic reticulum and Golgi apparatus were vacuolated, and secretory granules of varying optical density were visible (Fig. 2D).

Thyroid status of immature animals of group 3: TSH $0.14 \pm 0.02 \mu\text{IU/ml}$ ($p < 0.01$), T3 $3.36 \pm 0.33 \text{ nmol/l}$ ($p < 0.01$), T4 $50.14 \pm 5.73 \text{ nmol/l}$ ($p < 0.01$); in mature animals – $0.26 \pm 0.02 \mu\text{IU/ml}$ ($p < 0.01$), $2.06 \pm 0.18 \text{ nmol/l}$ ($p < 0.01$), $50.88 \pm 5.69 \text{ nmol/l}$ ($p < 0.01$), respectively. The cholesterol content on the 90th day of the experiment is: in immature rats $1.68 \pm 0.15 \text{ mmol/l}$ ($p < 0.01$), in mature rats – $1.49 \pm 0.14 \text{ mmol/l}$ ($p < 0.01$). Ioduria in immature animals of group 3 is $0.92 \pm 0.08 \mu\text{g/l}$, in mature animals – $1.54 \pm 0.14 \mu\text{g/l}$ ($p < 0.01$).

On the 90th day of the experiment, edema changes in the endocardium progressed. In light microscopy studies, the endocardium appeared as a veil-like strip covering the myocardium. In the light pink cytoplasm, flattened and weakly basophilic endothelial nuclei were visible (Fig. 3). The content of endothelin-1 in the blood of sexually immature animals increased by 5.7% ($p < 0.05$), while in sexually mature animals, it rose by 2.4% ($p < 0.05$).

Submicroscopically, the cytoplasm of endothelial cells exhibited medium electron density, with dilated membrane organelles and vacuoles present. The subendothelial layer was swollen and homogenized. Sarcoplasmic vacuolization of smooth muscle cells and edema of muscle-elastic fibers were noticeable.

The wall of the arteries also revealed edematous changes. Endothelial cells appeared flattened, and their nuclei were not identifiable throughout. The collagen-elastic framework of the media was deformed, and the coils of elastic fibers were uneven. Smooth muscle cell nuclei appeared misaligned and weakly basophilic. In certain fields of view, sarcoplasm appeared very light.

The adventitia exhibited edematous changes (Fig. 3C). Morphometric analysis showed an increase in wall thickness in the aorta, external carotid artery, and renal artery by 1.1% ($p < 0.05$), 1.3% ($p < 0.05$), and 1.0% ($p < 0.05$), respectively, in sexually immature animals. For sexually mature animals, the parameter increased by 0.6% ($p < 0.05$), 1.4% ($p < 0.05$), and 1.8% ($p < 0.05$), respectively.

In ultrastructural studies, flattened endothelial cells were observed on an indistinctly differentiated basal membrane, with a swollen subendothelial layer beneath. Similar edema changes were found in the fibers and smooth muscle cells of the artery wall (Fig. 3D).

In the prostate lobes on the 90th day of the experiment, edema changes were evident. Connective tissue fibers and smooth muscle cells in the stroma were swollen, accompanied by lymphocytic infiltration. The wall of the blood vessels was thickened, with stasis phenomena in the lumens. The epithelial cells of the terminal secretory sections showed signs of edema. The basal poles of their cytoplasm appeared clarified, with nuclei displaced. The apical light stained cytoplasm formed

a veil-like contour in the lumens of the terminal secretory sections (Figure 4).

The height of the epithelium in the terminal secretory sections of the ventral, dorsal lobes, and coagulating gland increased by 3.7% ($p < 0.05$), 4.3% ($p < 0.05$), and 3.9% ($p < 0.05$), respectively, in sexually immature animals. For sexually mature animals, the epithelial height increased by 1.2% ($p < 0.05$), 1.1% ($p < 0.05$), and 1.6% ($p < 0.05$), respectively.

During electron microscopy studies, in the epithelial cells deformed nuclei were visible due to the invagination of their nucleolemma. Membrane organelles were dilated and vacuolated. Mitochondria had clarified matrix and deformed cristae. Stasis phenomena were observed in the lumens of blood vessels, with vacuolized endothelial cell cytoplasm. Perivascular edema was prominent visualized. The sarcoplasm of smooth muscle cells exhibited a homogenized granular appearance.

In the adrenal glands, light-microscopic examination revealed edema changes in the capsule, cortex and medulla. Perivascular edema surrounding the vascular network was evident (Fig. 4C). The thickness of the adrenal cortex in sexually immature animals increased by 1.5% ($p < 0.05$). For sexually mature animals, it rose by 2.5% ($p < 0.05$).

Submicroscopically, stasis of formed elements of blood was observed. Cytoplasm of the endocrine cells contained mitochondria of different sizes with deformed cristae and light matrix. Membrane organelles of the synthetic apparatus were dilated and vacuolated, while secretory inclusions exhibited varying optical densities (Fig. 4D).

Edema changes were observed in all examined organs, progressing by the 90th day of the experiment. In both sexually immature and mature animals, an increase in endothelin-1, a vasoconstrictor exacerbating trophic disorders, was evident [16, 17, 18]. Edematous processes in the walls of elastic, mixed, and muscular-type arteries led to their thickening, confirmed by morphometric analysis [19, 20, 21]. Additionally, lipid profile changes served as a specific marker of hypothyroid conditions [22, 23, 24, 25, 26]. Edematous changes in the connective tissue components of the prostate and adrenal glands also compressed vascular structures, amplifying ischemic manifestations [27, 28]. Consequently, we observed edema-dystrophic changes in epithelial tissues.

The adrenal glands' involvement in lipid peroxidation due to their high content of unsaturated fatty acids in the plasmalemma of endocrine cells was noted [2]. Impaired thyroid hormone synthesis resulted in oxidative stress [10, 22, 29, 30], triggering a cascade of inflammatory and hemodynamic disturbances [31, 19, 32]. The prostate gland, containing key components of thyroid signaling, indicated potential direct action of thyroid hormones on this target organ [33]. Molecular iodine exhibited multi-factorial protective effects on the prostate, functioning as both a thyroid microelement and an antioxidant, anti-inflammatory agent, apoptosis inducer in pathological cells, and normalizer of prostate function in benign hyperplasia [7].




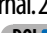


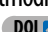
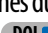

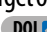
CONCLUSION

The level and degree of iodine deficiency is confirmed by ioduria indicators and thyroid profile. In all studied

organs, edema changes develop in all constituent structures already on the 60th day of simulated iodine deficiency, progressing to the 90th day of the experiment.

REFERENCES

1. Chakraborty A, Sarkar D, Dey P, Chandra AK. New insights into morphological, stereological and functional studies of the adrenal gland under exposure to the potent goitrogen thiourea. *Interdiscip Toxicol*. 2018;11(1):38–44. Available from: <https://doi.org/10.2478/intox-2018-0005> DOI
2. Egalini F, Marinelli L, Rossi M, Motta G, Prencipe N, Rossetto Giaccherino R, et al. Endocrine disrupting chemicals: effects on pituitary, thyroid and adrenal glands. *Endocrine*. 2022;78(3):395–405. Available from: <https://doi.org/10.1007/s12020-022-03076-x> DOI
3. Kukharchuk KhM. Clinical and epidemiological features of a subclinical hypothyroidism in young people. *Health of Society*. 2019;8(3):106–111. Available from: <https://doi.org/10.22141/2306-2436.8.3.2019.192174> Ukrainian DOI
4. Khmara T.V., Vlasova O.V., Bilyk Ya. O., Kryvchanska M. I., Vlasova K. V., Stravskyy Ya. S., Fedoniuk L. Ya. Features of prenatal morphogenesis and peculiarities of the utriculus prostaticus fetal anatomy // *Polski Merkuriusz Lekarski*. – 2023. – Vol. 51, issue 2. – P. 135–139.
5. Messina M, Redmond G. Effects of soy protein and soybean isoflavones on thyroid function in healthy adults and hypothyroid patients: A review of the relevant literature. *Thyroid*. 2006;16(3):249–258. Available from: <https://doi.org/10.1089/thy.2006.16.249> DOI
6. Otun J, Sahebkar A, Östlundh L, Atkin SL, Sathyapalan T. Systematic review and meta-analysis on the effect of soy on thyroid function. *Sci Rep*. 2019;9(1):3964. Available from: <https://doi.org/10.1038/s41598-019-40647-x> DOI
7. Aceves C, Mendieta I, Anguiano B, Delgado-González E. Molecular iodine has extrathyroidal effects as an antioxidant, differentiator, and immunomodulator. *Int J Mol Sci*. 2021;22(3):1228. Available from: <https://doi.org/10.3390/ijms22031228> DOI
8. Ryabukha O, Greguš M. Correlation analysis as a thyroid gland, adrenal glands, and liver relationship tool for correcting hypothyroidism with organic and inorganic iodine. *Procedia Comput Sci*. 2019;160:598–603. Available from: <https://doi.org/10.1016/j.procs.2019.11.041> DOI
9. Chandra AK, Mondal C, Sinha S, Chakraborty A, Pearce EN. Synergic actions of polyphenols and cyanogens of peanut seed coat (*Arachis hypogaea*) on cytological, biochemical and functional changes in thyroid. *Indian J Exp Biol*. 2015;53(3):143–151.
10. Asín J, Ramírez GA, Navarro MA, Nyaoke AC, Henderson EE, Mendonça FS, et al. Nutritional wasting disorders in sheep. *Animals (Basel)*. 2021;11(2):501. Available from: <https://doi.org/10.3390/ani11020501> DOI
11. Peixoto de Miranda ÉJF, Bittencourt MS, Pereira AC, Goulart AC, Santos IS, Lotufo PA, et al. Subclinical hypothyroidism is associated with higher carotid intima-media thickness in cross-sectional analysis of the Brazilian Longitudinal Study of Adult Health (ELSA-Brasil). *Nutr Metab Cardiovasc Dis*. 2016;26(10):915–921. Available from: <https://doi.org/10.1016/j.numecd.2016.06.005> DOI
12. Sampaio RAG, Riet-Correa F, Barbosa FMS, de Gois DD, Lima RC, da Silva IG, et al. Diffuse alopecia and thyroid atrophy in sheep. *Animals (Basel)*. 2021;11(12):3530. Available from: <https://doi.org/10.3390/ani11123530> DOI
13. Martínez-Galán JR, Pedraza P, Santacana M, Escobar del Ray F, Morreale de Escobar G, Ruiz-Marcos A. Early effects of iodine deficiency on radial glial cells of the hippocampus of the rat fetus. A model of neurological cretinism. *J Clin Invest*. 1997;99(11):2701–2709. Available from: <https://doi.org/10.1172/jci119459> DOI
14. Popadynets OH, Sahan OV, Barchuk RR, Voianskyi RS, Ananevych IM, Sahan NT, et al. Method for modeling iodine-deficient conditions with the addition of goitrogenic products. Patent of Ukraine No. 111647, 2016. Ukrainian.
15. Bahrii MM, Dibrova VA, Popadynets OH, Hryshchuk MI. Methods of morphological research: A monograph. Bahrii MM, Dibrova VA, editors. Vinnytsia: Nova Knyha; c2016. 328p. Ukrainian.
16. Baumgartner C, da Costa BR, Collet TH, Feller M, Floriani C, Bauer DC, et al. Thyroid function within the normal range, subclinical hypothyroidism, and the risk of atrial fibrillation. *Circulation*. 2017;136(22):2100–2116. Available from: <https://doi.org/10.1161/CIRCULATIONAHA.117.028753> DOI
17. Isailă OM, Stoian VE, Fulga I, Piraianu AI, Hostiuc S. The relationship between subclinical hypothyroidism and carotid intima-media thickness as a potential marker of cardiovascular risk: A systematic review and a meta-analysis. *J Cardiovasc Dev Dis*. 2024;11(4):98. Available from: <https://doi.org/10.3390/jcdd11040098> DOI
18. Semianiv M., Sydorchuk L., Fedonyuk L., Nebesna Z., Kamyshnyi O., Sydorchuk A., Vasiuk V., Dzhuryak V., Semianiv I., Sydorchuk R. Metabolic and hormonal prognostic markers of essential arterial hypertension considering the genes polymorphism AGTR1 (rs186) and VDR (rs2228570) // *Rom J Diabetes Nutr Metab Dis*. 2021; 3(28):284–291. 10.46389/rjd-2021-1042 DOI
19. Lindsay G, Bézie Y, Ragonnet C, Duchatelle V, Dharmasena C, Villeneuve N, et al. Differential stiffening between the abdominal and thoracic aorta: effect of salt loading in stroke-prone hypertensive rats. *J Vasc Res*. 2018;55(3):144–158. Available from: <https://doi.org/10.1159/000488877> DOI
20. Omid N, Khorgami M, Tajrishi FZ, Seyedhoseinpour A, Pasbakhsh P. The role of thyroid diseases and their medications in cardiovascular disorders: A review of the literature. *Curr Cardiol Rev*. 2020;16(2):103–116. Available from: <https://doi.org/10.2174/1573403X15666191008111238> DOI
21. Repchuk Y, Sydorchuk L, Fedoniuk L, Nebesna Z, Vasiuk V, Sydorchuk A, Iftoda O. Association of Lipids' Metabolism with Vitamin D Receptor (rs10735810, rs222857) and Angiotensinogen (rs699) Genes Polymorphism in Essential Hypertensive Patients. *Open Access Maced J Med Sci [Internet]*. 2021 Nov. 21 [cited 2021 Dec. 1];9(A):1052–6. <https://doi.org/10.3889/oamjms.2021.6975> DOI

22. Blum MR, Gencer B, Adam L, Feller M, Collet TH, da Costa BR, et al. Impact of thyroid hormone therapy on atherosclerosis in the elderly with subclinical hypothyroidism: A randomized trial. *J Clin Endocrinol Metab.* 2018;103(8):2988-2997. Available from: <https://doi.org/10.1210/jc.2018-00279> DOI 
23. Jung KY, Ahn HY, Han SK, Park YJ, Cho BY, Moon MK. Association between thyroid function and lipid profiles, apolipoproteins, and high-density lipoprotein function. *J Clin Lipidol.* 2017;11(6):1347-1353. Available from: <https://doi.org/10.1016/j.jacl.2017.08.015> DOI 
24. Pankiv VI, Yuzvenko TYu. Relationships of subclinical thyroid dysfunction and metabolic syndrome. *Clin Endocrinol Endocr Surg (Ukraine).* 2017;2(58):39-43. Available from: [https://doi.org/10.24026/1818-1384.2\(58\).2017.105577](https://doi.org/10.24026/1818-1384.2(58).2017.105577) Ukrainian. DOI 
25. Rauhulova T. Non-alcoholic fatty liver disease and hypothyroidism: review of clinical and experimental studies. *Galician Medical Journal.* 2021;28(4):E202142. Available from: <https://doi.org/10.21802/gmj.2021.4.2> goitrogenic products. Patent of Ukraine No. 111647, 2016. Ukrainian. DOI 
26. Skrypnyk NV. Metabolic syndrome and hypothyroidism: pathogenetic interrelations, diagnosis, and treatment. *Diabetology, Thyroidology, Metabolic Disorders.* 2017;1(37):60-63. Ukrainian.
27. Fedoniuk LYa, Nesteruk SO, Hnatiuk MS, Smachylo II, Tverdochlib VV, Yakymchuk OA. Quantitative morphological features of the structural rearrangement of the venous blood vessels of the prostate gland in post-resection portal hypertension. *Polski Merkuriusz Lekarski.* 2023; 6(51):608-612. <https://doi.org/10.36740/Merkur202306105> DOI 
28. Hnatiuk M. S., Nesteruk S. O., Fedoniuk L. Ya., Yakymchuk O. A., Smachylo I. I., Tverdochlib V. V. Quantitative morphological analysis of age structural changes in prostate of experimental animals with ethanol poisoning // *Wiadomości Lekarskie.* – 2024. – Vol. 77 (2). – P. 268-272. doi: 10.36740/WLek202402112 DOI 
29. Hlozhyk IZ. Biochemical markers of free radical oxidation and lipid exchange in rats with obesity, iodine deficiency and obesity in combination with iodine deficiency. *Ukrainian Journal of Medicine, Biology and Sports.* 2021;6(4):166-171. Available from: <https://doi.org/10.26693/jmbs06.04.166> Ukrainian. DOI 
30. Moog NK, Entringer S, Heim C, Wadhwa PD, Kathmann N, Buss C. Influence of maternal thyroid hormones during gestation on fetal brain development. *Neuroscience.* 2017;342:68-100. Available from: <https://doi.org/10.1016/j.neuroscience.2015.09.070> DOI 
31. Fabricio MF, Jordão MT, Miotto DS, Ruiz TFR, Vicentini CA, Lacchini S, et al. Standardization of a new non-invasive device for assessment of arterial stiffness in rats: Correlation with age-related arteries' structure. *MethodsX.* 2020;7:100901. Available from: <https://doi.org/10.1016/j.mex.2020.100901> DOI 
32. Denefil O. V., Druziuk R. B., Medynskiy M. I., Fedoniuk L. Ya., Nebesna Z. M. The peculiarities of biochemical and morphological changes in the heart of the castrated rats in the development of adrenalin damage of heart // *Wiadomości Lekarskie.* – 2023. – Vol. 76 (2). – P. 274-284.
33. Anguiano B, de Oca CM, Delgado-González E, Aceves C. Prostate gland as a target organ of thyroid hormones: advances and controversies. *Endocr Connect.* 2022;11(2):e210581. Available from: <https://doi.org/10.1530/EC-21-0581> DOI 

The study is carried out within the framework of the initiative research work of the Department of Human Anatomy at Ivano-Frankivsk National Medical University "Ontogenetic Peculiarities of the Morpho-functional State of Organs and Tissues in Iodine Deficiency and Hypothyroidism" (0119U002847).











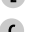

CONFLICT OF INTEREST

The Authors declare no conflict of interest

CORRESPONDING AUTHOR

Oksana Popadynets
Department of Human Anatomy
Ivano-Frankivsk National Medical University
Tel. +38(067)3999143
E-mail: Fedonyuk22Larisa@gmail.com

ORCID AND CONTRIBUTIONSHIP

Liliia V. Sobol – orcid 0000-0002-9750-3493   
Ivan S. Kuibida – orcid 0009-0007-1534-2213   
Oleksandra T. Harhaun – orcid 0009-0004-1437-8941   
Oksana H. Popadynets – orcid 0000-0002-2093-5984   

 – Work concept and design,  – Data collection and analysis,  – Responsibility for statistical analysis,  – Writing the article,  – Critical review,  – Final approval of the article

RECEIVED: 10.05.2025

ACCEPTED: 07.09.2025

